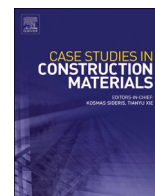


Contents lists available at [ScienceDirect](https://www.sciencedirect.com)

Case Studies in Construction Materials

journal homepage: www.elsevier.com/locate/cscm

Effect of cassava starch, hydrated lime, and carboxymethylcellulose on the physicomechanical behavior of mixtures with clay matrix

Oswaldo Hurtado-Figueroa^{a,c,*}, Alfonso Cobo Escamilla^a, Humberto Varum^b, Romel J. Gallardo Amaya^c

^a Escuela Técnica Superior de Edificación, Universidad Politécnica de Madrid—UPM, Madrid 28040, Spain

^b CONSTRUCT-LESE, Departamento de Engenharia Civil, Faculdade de Engenharia da Universidade do Porto, FEUP, Porto 4200-465, Portugal

^c Grupo de Investigación en Construcción, Geotecnia y Medio Ambiente—GIGMA, Universidad Francisco de Paula Santander Ocaña—UFPSO, Ocaña 546552, Colombia

ARTICLE INFO

Keywords:

Cassava starch
Hydrated lime
Clay
Carboxymethylcellulose
Mechanical strength

ABSTRACT

The physical and mechanical behavior of experimental mixtures with additions of cassava starch, carboxymethyl cellulose, and hydrated lime in a clay matrix is described. The added elements accounted for 3% of the weight of the mixes and the clay matrix for 97%. Mixing water was incorporated in different % according to the workability and molding of the mixes. Tests indicated the influence of additions on volumetric changes, particle detachment, and mechanical strength of the experimental mixtures. It was concluded that percentages $\geq 50\%$ carboxymethylcellulose favored properties in mixtures. The opposite result was obtained with the addition of lime. Mixtures with additions of 25% cassava starch and 75% carboxymethylcellulose reported similar mechanical behavior and no particle detachment.

1. Introduction

The current environmental problems motivate the implementation of actions to mitigate the damage caused to ecosystems due to the generation of waste and emissions of polluting gases. For this reason, productive sectors are developing alternative materials whose production is environmentally friendly [1].

Abbreviations: Adobe, Earth Brick; AL, Atterberg Limits; Al, Aluminum; C, Carbon; CAS, Cassava Starch; Cg, Carboxymethylether group; CHF, Chemical Formula; CL, Clay; CM, Control Mixture; CMC, Carboximethylcellulose; CMX, Clay Matrix; CS, Compressive Strength; DC, Degree of Chalking; Dd, Dense areas; DOE, Design of Experiments; DS, Drying Shrinkage; DW, Distilled Water; DY, Density; EDS, Energy Dispersive X-ray Spectroscopy; EMS, Experimental Mixtures; F, Fissures; FS, Flexural Strength; FTIR, Fourier-transform infrared spectroscopy; GMAS S.A.S, Geology, Geochemistry and Geophysics Laboratory; Gr, Glucopyranose rings; Hd, Homogeneously dispersed; INV E, Instituto Nacional de Vías; Kg, Kilograms; LABMAC, Laboratory of Analysis of Materials for Construction; LaC-GMC, Characterization Laboratory of the Composite Materials Group; LG, Laser Granulometry; LM, Hydrated Lime; LV, Lost volume; MA, Moisture Absorption; MCM, Mixtures with a clayey matrix; MW, Mixing Water; NTC, Norma Técnica Colombiana; O, Oxygen; P, Pores; Pa, Porous areas; PC, Portland Cement; Ps, Particle separation; Pt, Portlandite; PZ, Particle size; SEM, Scanning Electron Microscopy; SENA, Servicio Nacional de Aprendizaje; Si, Silica; SP, Sample; Us, Undulations; USCS, Unified Soil Classification System; XRD, X-Ray Diffraction; XRF, X-Ray Fluorescence; %wt, %/weight.

* Corresponding author at: Escuela Técnica Superior de Edificación, Universidad Politécnica de Madrid—UPM, Madrid 28040, Spain.

E-mail address: os.hurtado@alumnos.upm.es (O. Hurtado-Figueroa).

<https://doi.org/10.1016/j.cscm.2024.e03022>

Received 15 January 2024; Received in revised form 18 February 2024; Accepted 27 February 2024

Available online 29 February 2024

2214-5095/© 2024 The Authors. Published by Elsevier Ltd. This is an open access article under the CC BY-NC-ND license (<http://creativecommons.org/licenses/by-nc-nd/4.0/>).

Such is the case of the construction industry, a sector that generates considerable environmental pressure due to the use of non-renewable resources and energy consumption in its processes [2]. The use of resources by the construction industry is directly proportional to the increase in population on the planet, a situation that further aggravates the worrying environmental problems [3].

For this reason, researchers in the construction industry have decided to take a look back to implement ancestral materials and construction techniques in modern projects [4]. In this regard, Rammed earth, Earth brick (Adobe), Cob, wattle, and daub inspire researchers to use earth as an alternative material based on the constructive and environmental advantages of this natural material [5].

Environmental advantages are reflected in the zero or minimal carbon footprint generated by the use of the earth as a building material. Constructive advantage that allows the reuse of soil from demolition processes by simply moistening and mixing it. The proposal presented as a sustainable alternative to the problems generated by climate change [6].

These ancestral construction techniques of which earth is the main material have been automated through the implementation of advanced construction methods that include digital Industry 4.0 processes. Modern processes aim to generate environmental awareness through the implementation of a material whose vestiges have demonstrated the importance of the earth as a building material throughout the history of mankind [7].

Some research aims to reduce the carbon footprint generated in the production of conventional building materials and elements in which the use of fossil fuels is necessary for the combustion process in their manufacture. Energy expenditure is common practice in the extraction, processing, and manufacturing of raw materials that are transformed into cementitious materials and construction elements [8].

For this reason, the increase in the physical-mechanical behavior of clay matrix mixtures (MCM) used in old constructions has attracted the interest of researchers to substitute conventional materials for those used in old constructions. Several methods of stabilization of MCM have been implemented, of which the addition of % Portland Cement (PC) is the most representative [9].

However, the process for the manufacture of PC provides minimal environmental contributions in experimental mixtures (EMS) due to the considerable energy costs required for its manufacture, which emit between 5% and 8% of the CO₂ emissions generated worldwide [10].

Hydrated lime (LM) was used to stabilize MCM in the manufacture of adobes, reporting an increase in compressive strength (CS) between 40% and 50% [11]. As with the use of PC, LM additions in larger quantities do not represent positive environmental contributions due to the generation of CO₂ in its production. Studies indicate that the production of 1 kg (kg) of LM emits 1.2 kg CO_{2eq} compared to the production of 1 kg of PC which emits 0.9 kg CO_{2eq} [12].

Some research combined CP with ash from agricultural rice residues to improve the mechanical properties of clay matrix blocks (CMX). It was reported that additions of 4–8% of PC and 5–10% of ash obtained favorable results in CS [13]. However, the processing to obtain the ash could generate a carbon footprint similar to or greater than that of the PC. However, the half-life of the CO₂ emitted by biomass combustion is shorter. Characteristic that depends on how the plant material is grown [14].

Similar research included concrete dust from demolition and construction waste at MCM. PC was also incorporated in different %. It was concluded that the addition of concrete powder at 20% and PC at 8% obtained increases in the mechanical behavior of EMS [15]. However, the process for obtaining the concrete powder requires considerable energy costs. Energy costs described in the crushing, grinding, and mixing process can exceed 3 kW to obtain only 3.5 kg of material. This implies high energy costs to obtain 1m³ of material [16].

Even when sustainable alternatives are presented through the use of alternative materials, the processing and transformation of these elements can have considerable environmental impacts. As described in the research conducted by Sadok et al., where the use of calcined sediments in the production of PC emitted 935.10 kg CO_{2eq}/T, which represents a reduction of 3.74% compared to other processes [17].

On the other hand, studies carried out on unstabilized compressed soil blocks refer to the improvement of the granulometry of the clayey soil to improve the CS of the EMS. It was concluded that by modifying the granulometric curve, it is possible to increase the mechanical properties of EMS. Modification is carried out by mixing different clay soils or with the addition of sand [18]. Environmentally friendly experimental feature due to the reuse of soil after demolition of structures.

Similar research incorporates straw [19] and sawdust in MCM in EMS for adobe production. Results concluded that straw and sawdust incorporations of 30% by volume significantly improve mechanical properties [20]. The research proposes the incorporation of agricultural and industrial wastes in MCM following the production and consumption model of the circular economy [21].

Minimizing environmental impact through the life cycle assessment of materials would improve production systems by enabling a comprehensive assessment of the carbon footprint of building materials. In this sense, the life cycle assessment of materials can be used to promote the circular economy in the construction industry [22].

With the above, the present research article proposes the improvement of the physicomechanical properties of MCM through the addition of Cassava Starch (CAS), Carboxymethylcellulose (CMC), and LM in a small %. Organic and inorganic additions, the results of which significantly improve the mechanical behavior of EMS.

The EMS are presented as a sustainable alternative for their implementation as substitute materials in modern construction projects, mitigating the environmental pressure exerted by the processes inherent in the extraction, transformation, and production of conventional materials, of which PC is presented as a construction material with a large carbon footprint.

Fig. 1 illustrates comparatively the life cycle of conventional building materials and soil used as building materials.

The figure shows the extraction and processing of natural resources—processes requiring considerable energy costs to produce construction elements. The implementation and demolition of the materials at the end of the useful life of the buildings are shown. As for conventional materials, the recovery process is shown, which requires a series of activities requiring energy costs. However, the construction techniques and the properties of the materials used in earth construction simplify processes allowing the direct reuse of

earth for the elaboration of construction materials. In the same way, the soil can be reincorporated into nature after the demolition of built structures. Environmental characteristic that identifies the circularity of the material with minimal or no impact on ecosystems.

2. Materials and methods

2.1. Materials

The research was carried out by making control mixtures (CM) and EMS mixtures with CMX. The CM contained 100% of its weight (%wt) in clay (CL). EMS contained 97%wt of CL and 3%wt in additions of LM, CAS, and CMC. The preparation of mixtures counted with the addition of different % of distilled water (DW) used for mixing.

2.1.1. Clay

The CL was taken from a local company dedicated to the manufacture and commercialization of ceramic products for the construction industry. The CL used in the manufacture of test samples (SP) was recovered after the milling process carried out by the company to produce extruded blocks and tiles.

Fig. 2 shows the recovery process of CL. The natural state of the CL is shown in Fig. 2a. The process of grinding and routing by the conveyor belt Fig. 2b. Collection Fig. 2c. Packaging Fig. 2d.

2.1.2. Hydrated lime

LM is a product commonly used as a cementitious material and as a main element for the elaboration of different materials and construction elements [23]. The LM used in the EMS was purchased from a local marketer.

2.1.3. Cassava starch

Cassava is the root of a shrub of the Euphorbiaceae family from which starch with high nutritional content is extracted. Cassava is part of the staple diet of millions of people in America, Africa, and Oceania. CAS is also commonly used in the manufacture of paper and cardboard due to its binding properties [24]. The CAS used in the research was purchased from a food products trader.

2.1.4. Carboxymethylcellulose

CMC is an organic compound derived from cellulose. Its main characteristic is its ability to be soluble in contact with water. CMC is used as a thickener and stabilizer in blends. It is also used in different industries such as food, pharmaceuticals and recently in research aimed at cleaning wastewater in the textile industry [25]. As with CAS, CMC was purchased from a local food retailer.

Fig. 3 shows the components used in the EMS. The CL is shown Fig. 3a. LM Fig. 3b. CAS Fig. 3c. CMC Fig. 3d.

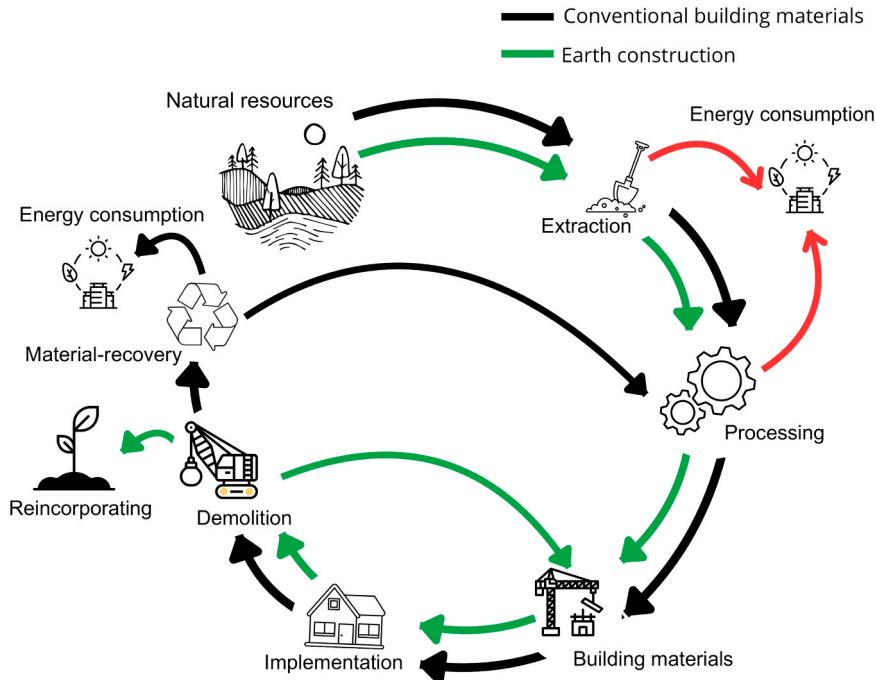


Fig. 1. Life cycle of conventional building materials and soil used as building materials.

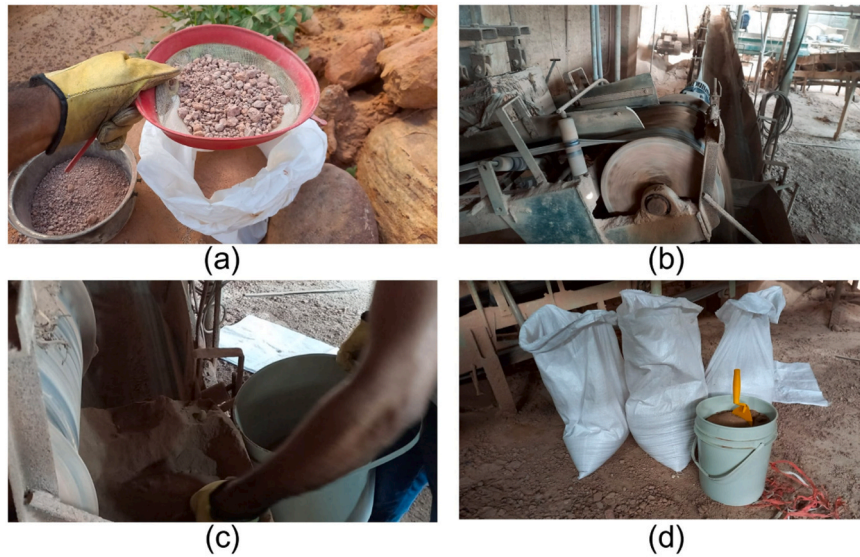


Fig. 2. Collection of CL.

2.2. Methods

2.2.1. Physical characterization

The laser particle size test (LG) was performed due to the small particle size (PZ) of the EMS components. Test performed by the Characterization Laboratory of the Composite Materials Group (LaC-GMC) of the Universidad del Valle - Colombia by application of the wet laser diffraction method in compliance with the International Organization for Standardization 13320 (ISO-13320) [26]. The equipment used was the Mastersizer 2000 particle size analyzer, working range (0.02–2000 microns).

The CL was subjected to particular characterization tests. Its liquid limit was determined by means of the Atterberg Limits (AL). Test performed under the E125–13 standard of the Instituto nacional de Vías (INV E 125–13) [27]. The plastic limit and plasticity index of the soils were tested INV E 126–13 [28]. The tests were carried out at the Construction Materials Analysis Laboratory (LABMAC). Laboratory located in the Servicio Nacional de Aprendizaje (SENA) de la Regional Norte de Santander - Colombia.

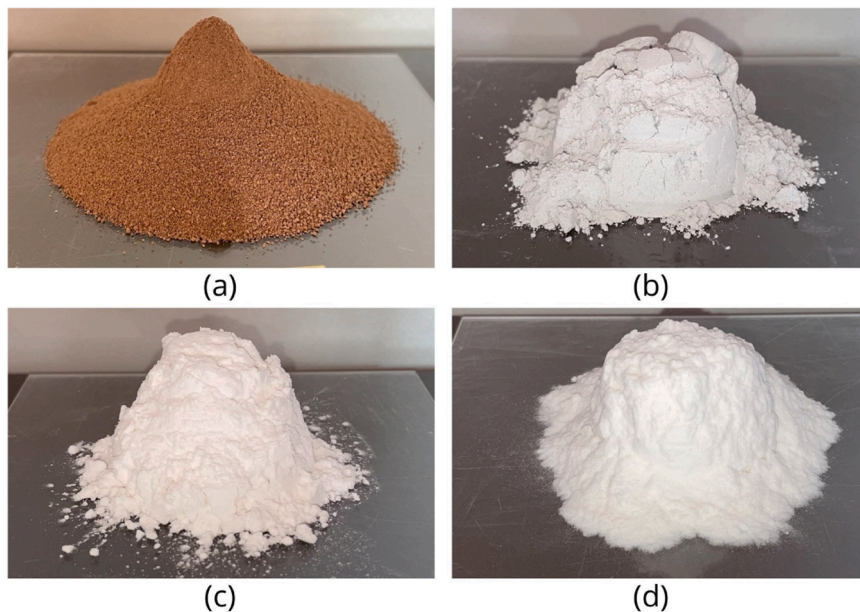


Fig. 3. EMS components.

2.2.2. Chemical characterization

The chemical composition of CL and LM was identified by the X-Ray Fluorescence (XRF) pellet or bead preparation method. The equipment used was the PANalytical AXIOS Max wavelength dispersive X-ray fluorescence spectrometer (WDXRF). Test performed by LaC-GMC.

2.2.3. Mineralogical characterization

The quantification of minerals from the CL and LM was performed by means of mineral identification and quantification assay by X-Ray Diffraction (XRD) powder assembly. The equipment used was the Bruker D4 Endeavor diffractometer. Test performed by Geology, Geochemistry and Geophysics Laboratory (GMAS S.A.S) – Colombia.

Due to the organic nature of CAS and CMC, their physicochemical characterization was performed by applying the Fourier transform infrared spectroscopy method (FTIR). Test performed with Spectrum 100, PerkinElmer. Working range (450 cm⁻¹–4000 cm⁻¹). Analysis performed in the LaC-GMC laboratory.

2.2.4. EMS design

Two types of mixtures, CM and EMS, were elaborated in the research. The EMS consisted of 4 components CL, LM, CAS, and CMC. The CL constituted the CMX and the LM, CAS and CMC were part of the additions. CM was performed with 100%wt of CL with addition of mixing water (MW) corresponding to 25%wt of the mixture.

The EMS were designed using Minitab statistical software. The Simplex Lattice Design of Experiments (DOE) tool was used for the design. Design relating the simultaneous and individual inclusion of the 3 additions LM, CAS and CMC, with reticulum grade 4. The design consisted of 3 randomized replicates. The %wt of the CL in the EMS was the processing constant.

In summary, 100%wt of the EMS was comprised of 97%wt of CL and 3%wt of additions. DOE distributed 3%wt of the mixture in additions comprising 0%wt, 25%wt, 33.3%wt, 50%wt, 75%wt, and 100%wt. Resulting in 16 EMS with 3 replications. This adds up to 48 EMS SP and 3 CM SP for each CS, FS and DC test. For the CS test, an additional test SP was used to determine the moisture absorption (MA). A total of 170 test SP were made.

2.2.5. Mixing process

The mixing of components in EMS was carried out according to their combinations. For EMS containing LM, manual dry mixing of CL and LM was performed. EMS with additions of CAS and CMC were dissolved in MW. The MW temperature for CAS dissolution was $60 \pm 5^\circ\text{C}$. The MW temperature for CMC dissolution was $35 \pm 5^\circ\text{C}$.

The MW was added in different quantities for each EMS to determine the optimum content that would facilitate workability and allow molding, taking as a reference the research conducted by Lagouin et al., where it was indicated that the typology of the materials conditions the addition of the % of MW [29]. As in the CM, the MW was incorporated in %wt total EMS. Mixing of the EMS was carried out mechanically for 10 minutes.

Table 1 shows the 16 DOE-designed EMS. The EMS are listed along with the random number of the run. The % distribution of the components in the mixtures is recorded. The %wt of addition corresponding to each of the components is indicated. The %wt of MW is indicated. Additions totaled 3%wt of the mixture. CL totaled 97%wt of the mixture.

Fig. 4 shows the EMS mixing process. Manual dry blending of CL and LM Fig. 4a. MW temperature control for dissolving CAS and CMC Fig. 4b. Mechanical mixing process Fig. 4c.

Table 1
DOE – EMS.

EMS	Components				MW %/wt
	97%/wt	3%/wt			
		%/wt Additions	LM	CAS	
EMS-48	CL	33,3	33,3	33,3	45
EMS-21		50	25	25	60
EMS-15		-	-	100	60
EMS-38		50	-	50	55
EMS-41		25	25	50	45
EMS-28		-	75	25	35
EMS-35		75	-	25	35
EMS-45		-	50	50	40
EMS-30		-	25	75	40
EMS-2		75	25	-	30
EMS-42		25	-	75	50
EMS-4		50	50	-	25
EMS-39		25	75	-	30
EMS-11		-	100	-	25
EMS-24		25	50	25	35
EMS-33		100	-	-	20

2.2.6. Test samples preparation

Three types of SP were made. I) Cylindrical SP [30] 10 cm in diameter and 2.54 cm high to determine density (DY), drying shrinkage (DS), volume loss (LV) and degree of chalking (DC). The latter, as established by the Norma Técnica Colombiana 1457–6 (NTC 1457–6) [31]. II) 5 cm side cubic SP to evaluate the CS according to NTC 220 [32]. With these SP, the capillary MA test was carried out by placing the SP on an absorbent sponge for one hour, a method performed by Maria Costi de Castrillo et al., [33]. III) Prismatic SP of 16 cm*4 cm*4 cm to evaluate flexural strength (FS) according to NTC 120 [34].

Fig. 5 shows the SP made in the investigation. Cylindrical SP Fig. 5a. Cubes and prisms Fig. 5b. Set of SP Fig. 5c.

2.2.7. Physical and mechanical tests

The DY, LV, DS and DC of the CM and EMS were evaluated with the cylindrical SP. DY, LV and DS were measured daily up to day 40. The average of 8 measurements of the diameter and thickness of each SP was taken. The DC test was performed according to NTC 1457–6. With the DC test, particle detachment could be identified.

The cubic SP were tested to determine the CS. Also evaluated was the % of MA. The Prismatic SP were used to evaluate the FS. DC, CS and FS tests were performed after 40 days of drying at room temperature. This drying time was proposed based on the research conducted by Khorasani & Kabir [35].

Fig. 6 shows the control of DY, LV and DS of the CM and EMS Fig. 6a. The DC test Fig. 6b. MA Fig. 6c. CS Fig. 6d. FS Fig. 6e.

2.2.8. Microscopic observation

Surface observation and characterization by scanning electron microscopy (SEM) was performed to evaluate the morphology and interaction of particles between components. Simultaneously, energy dispersive X-ray spectroscopy (EDS) mapping was performed,

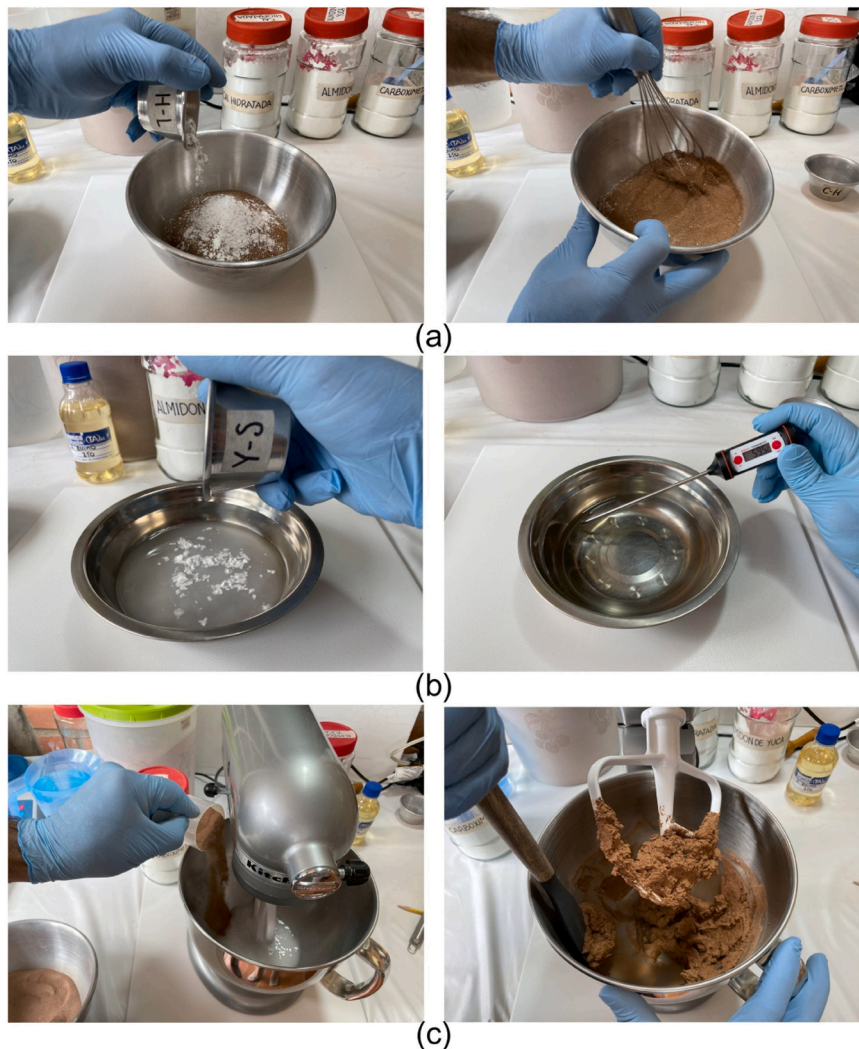


Fig. 4. EMS elaboration process.

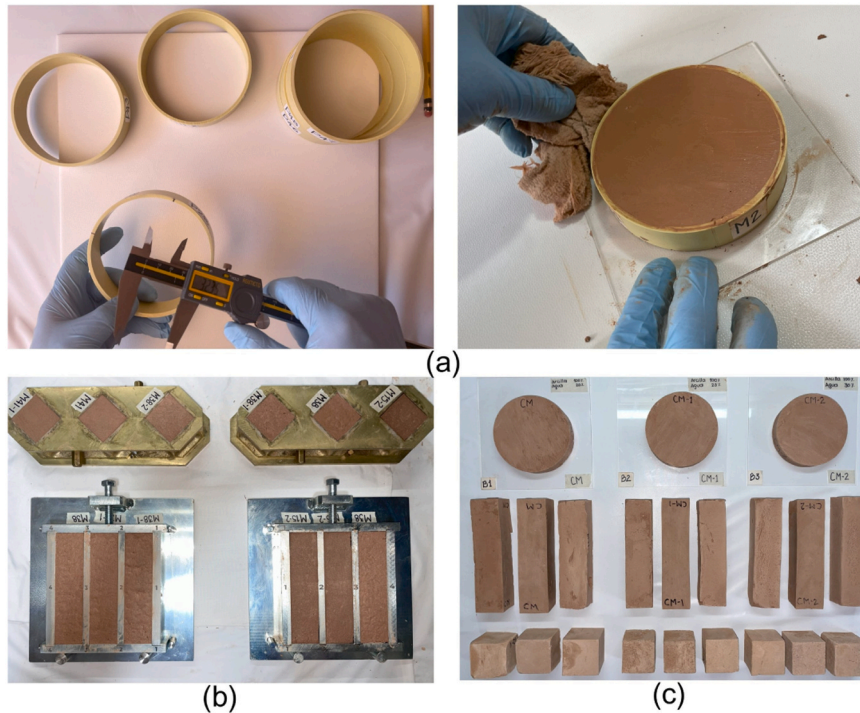


Fig. 5. Samples produced.

which allowed the elemental chemical characterization of the samples.

Fig. 7 presents the SEM and EDS evaluation of the CM and EMS. The basic SEM observation is shown in Fig. 7a. EDS mapping Fig. 7b. Elemental chemical composition and distribution Fig. 7c.

Fig. 8 shows the flow diagram carried out in the research, which graphically represents the system of procedures and activities developed.

3. Results and discussion

3.1. Laser granulometry

The LG determined the particle size composition by evaluating the PZ in the EMS components. The CAS obtained the lowest % corresponding to the average diameter of PZ with 15.20 microns (μm). In contrast, CMC had the highest % with 89.27 μm . AS was considered as the finest material of which 90% of the average PZ 22.49 μm . However, the CL had the smallest PZ with 0.15 μm .

PZ identification of the components was able to determine the manageability and solid-state phenomena of the EMS. However, some research questions this type of evaluation in MCM CS and FS because it only focuses on PZ analysis [36].

Table 2 summarizes the percentage distribution of the PZ corresponding to the 4 EMS components. The PZ is recorded in μm . $d(0,1)$ is recorded as the PZ below which 10% of the analyzed sampling remains. $d(0,5)$ is recorded as the PZ at which 50% of the analyzed sampling is below and 50% is above. $d(0,9)$ is recorded as the PZ below which 90% of the analyzed sampling remains. $D(4,3)$ is recorded as the mean diameter of the distribution, considered in volume.

Fig. 9 shows the particle-size curves presented by the PZ of the components. CL Fig. 9a. LM Fig. 9b. CAS Fig. 9c. CMC Fig. 9d.

3.2. Atterbreg limits

The liquid limit of the CL yielded 43%. The liquid limit is the moisture content above which the soil behaves as a viscous liquid. This makes it possible to control the mixing water for MCM. The plastic limit yielded 13%. The plastic limit is the moisture content below which the soil behaves as a solid. It allows for predicting the behaviour of the mixture concerning its DS. The plasticity index yielded 30%. The plasticity index is a range of consistency in which the soil presents plastic properties. It establishes criteria for the selection of the clay material concerning the final consistency of the mixture for moulding [37]. According to the Unified Soil Classification System (USCS) which classifies clays according to the % of their liquid limit, the CL used in the research is classified as low plasticity CL because its liquid limit is less than 50%. A characteristic that favoured the research because soils with a higher plasticity value are characterized by low compressive strength, inadequate durability, and excessive DS [38].

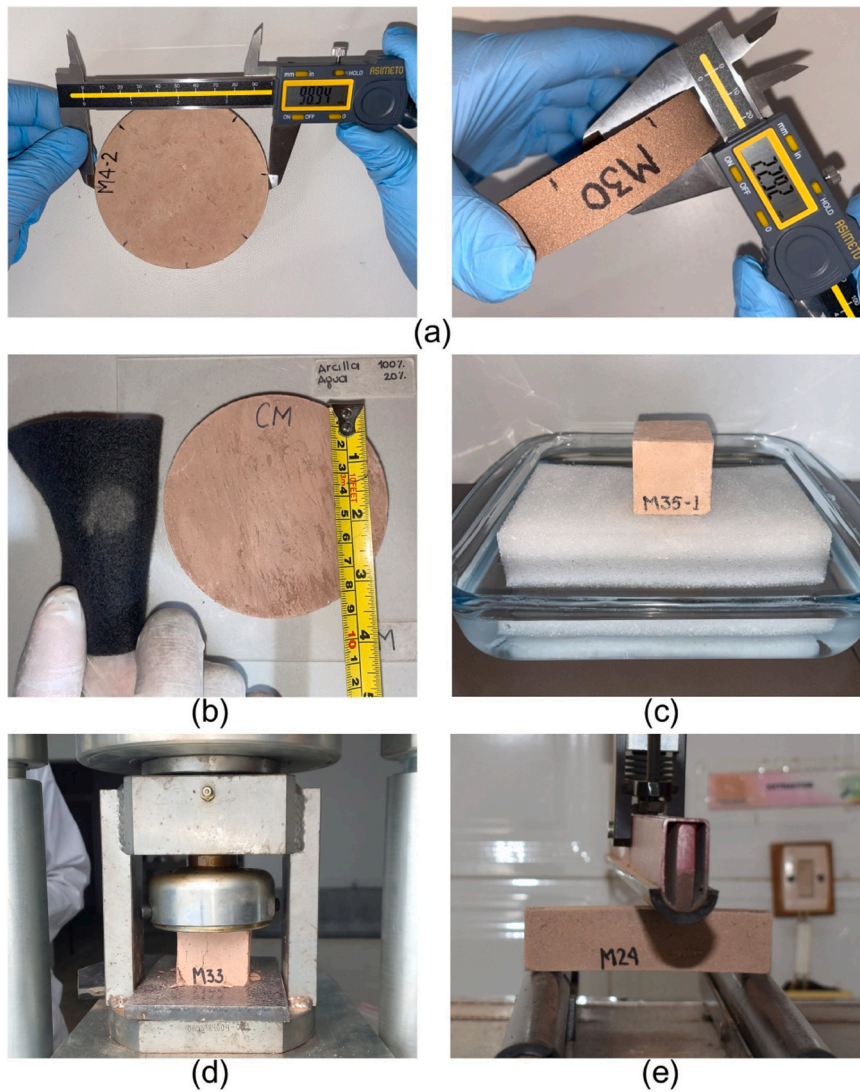


Fig. 6. CM and EMS physical tests.

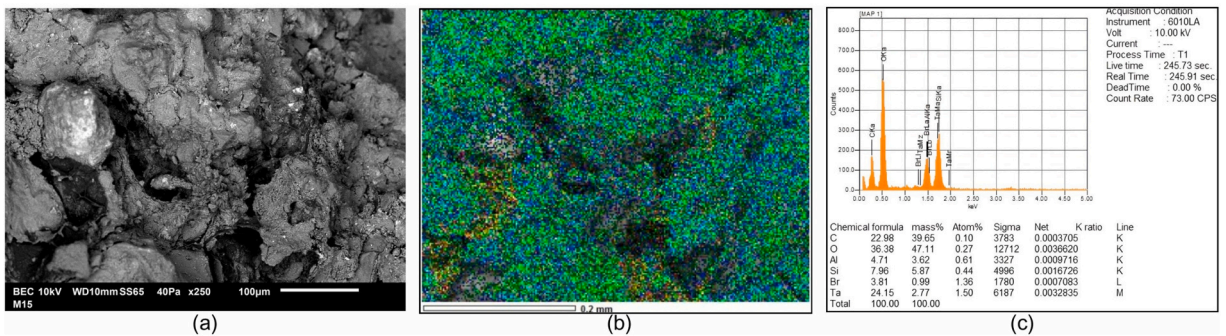


Fig. 7. SEM & EDS.

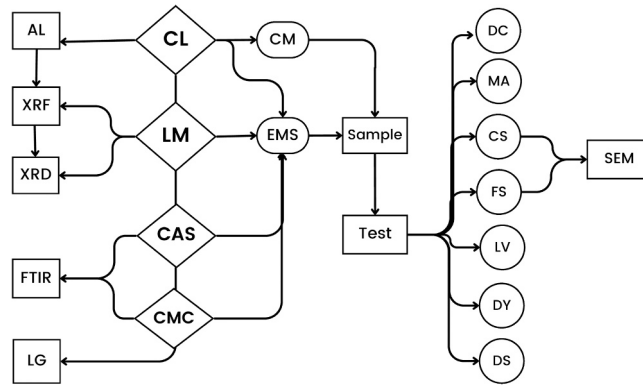


Fig. 8. Flow diagram.

Table 2
PZ components.

Component	d(0,1) µm	d(0,5)	d(0,9)	D(4,3)
CL	0,15	5,07	54,09	21,77
LM	3,12	10,84	125,87	42,67
CAS	9,03	14,39	22,49	15,20
CMC	23,06	58,33	184,38	89,27

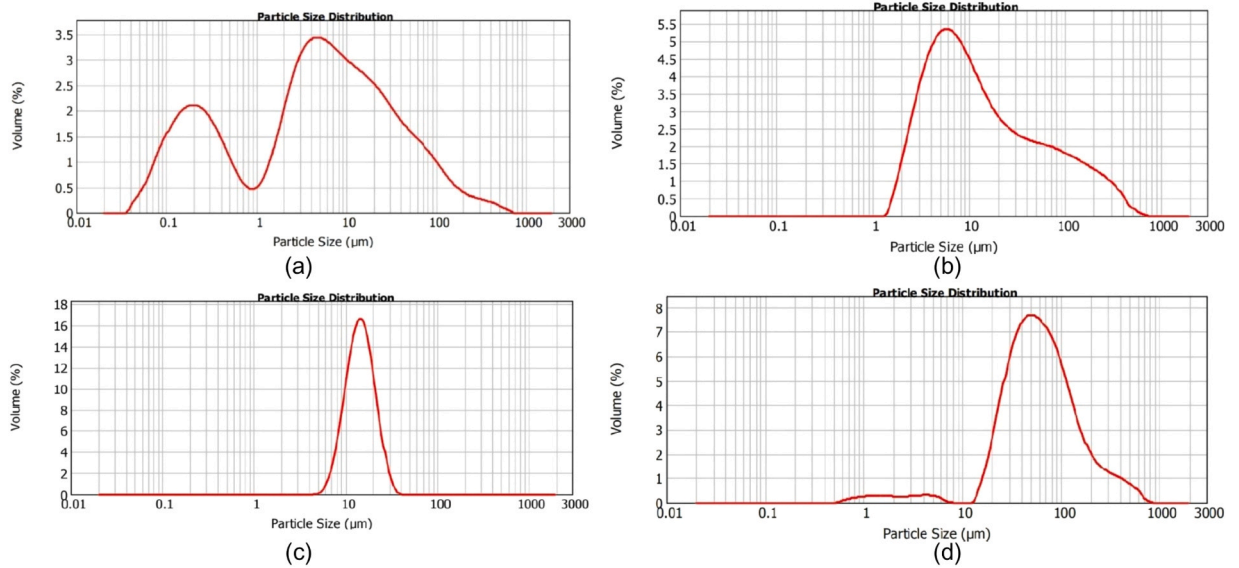


Fig. 9. Component PZ distribution.

Table 3
Chemical composition LM & CL.

Component	Chemical Composition										
	LOI	Na ₂ O	MgO	Al ₂ O ₃	SiO ₂	P ₂ O ₅	SO ₃	K ₂ O	CaO	TiO ₂	Fe ₂ O ₃
LM	20,49	0,01	1,89	1,30	5,52	0,02	1,44	0,06	68,56	0,11	0,70
CL	6,02	0,11	0,70	20,23	65,08	0,14	0,09	1,56	0,16	0,88	4,86

3.3. XRF

The chemical composition of the elements present in the CL and LM was described in the form of oxides. Due to the nature of the LM, CaO was the element with the highest % presence. Na₂O and P₂O₅ were shown in lower %. In the CL, SiO₂ and Al₂O₃ were the elements with the highest presence, exceeding 80%. Characteristic that places CL in the group of aluminosilicates [39].

Table 3 presents the chemical composition of the CL and the LM. Results presented in %wt of each element in 100 g of analyzed sampling. LOI corresponds to the % of analyzed sampling lost by ignition at 1000° C at 1 hour of exposure. In order to allow better visualization, the elements Cl, Cr₂O₃, MnO, ZnO, Rb₂O, SrO, ZrO₂, BaO were not listed in the table because the % of presence was ≤ 0.05 in the two components.

3.4. XRD

Mineralogical identification pointed out Quartz as the mineral present in the LM and the CL. The mineral with the highest presence in the LM was Portlandite with 49%.

Quartz is a fundamental mineral for obtaining high properties of fired bricks due to its interaction with silica, which increases the melting rate of minerals during combustion. However, high quartz contents in MCM reduce the clay plasticity due to its characteristic as a non-clay mineral [40]. Portlandite is the result of the hydration of lime. It is a calcium hydroxide that when interacting with silica allows particle cohesion of the resulting mixture [41]. Consequently, high portlandite content in lime decreases the DS in mixtures.

Table 4 shows the mineralogical composition of the LM and the CL. The mineral, the chemical formula (CHF), and the %/wt of mineral in 100 g of analysed sampling are identified.

Fig. 10 shows the diffractograms of the CL and LM. The peak corresponding to Portlandite, a representative mineral in the LM, can be seen Fig. 10b. Similarly, the peak of quartz, an abundant mineral CL is shown in the Fig. 10a. Quartz is identified as the mineral present in the 2 components.

3.5. FTIR

FTIR test was performed on CMC and CAS in their natural state to identify the main functional groups in these organic components added to the EMS.

Fig. 11 presents the FTIR spectra of the CMC and CAS. In the FTIR spectrum of the CMC sample, the functional groups characteristic of its chemical structure can be identified with bands at 1598,54 cm⁻¹ corresponding to the carboxymethylether group (Cg). A strain band of the -OH group is displayed at a wavelength of approximately 3433,81 cm⁻¹ and a band corresponding to the stretching vibration of -CH₂- at 2923,22 cm⁻¹. Group confirmed by the signal at 1430,99 cm⁻¹ assigned to the scissors motion of the -CH₂- group. These identified grouping are characteristic of CMC Fig. 11a.

With the FTIR spectrum of CAS it was possible to identify the available functional groups. Peaks A and B attributed to the C-C stretching of the glucopyranose rings (Gr) that compose the amylose and amylopectin present in the CAS are shown. Band 1648,94 relates the O-H and N-H deformation of the primary amine [42]. The bands observed at 2932,62 cm⁻¹ and 3366,86 cm⁻¹ correspond to the C-H stretching vibration of the aliphatic groups and the O-H stretching of the glucopyranose rings. Characteristic attributed to polysaccharides such as cellulose and starch [43] Fig. 11b.

3.6. Degree of chalking

Using as a guide the photographic reference standard number 1 applied for method A of NTC 1457–6, the DC of the CM and EMS were determined. Photographic pattern shows 4 DC. I) No 8, indicates that the SP did not show particle detachment. II) No 6, slight DC. III) No 4, moderate DC. IV) No 2, considerable DC. In this sense, DC No. 8 indicates no particle detachment and DC No. 2 indicates higher particle detachment.

Table 4
Mineralogical composition LM and CL.

LM			CL		
Mineral	CHF	% /wt	Mineral	CHF	% /wt
Quartz	SiO ₂	11	Quartz	SiO ₂	77
Calcite	CaCO ₃	10	K-Feldspar	KAlSi ₃ O ₈	<1
Dicalcium Silicate	Ca ₂ SiO ₄	6	Anatase	TiO ₂	1
Tricalcium Aluminate	Ca ₃ Al ₂ O ₆	2	Hematite	Fe ₂ O ₃	2
Free Lime	CaO	1	Pyrite	FeS ₂	1
Portlandite	Ca(OH) ₂	49	Kaolinite	Al ₂ Si ₂ O ₅ (OH) ₄	16
Xonotlite	Ca ₆ Si ₆ O ₁₇ (OH) ₂	3	Illite-Mica	KAl ₂ ((OH) ₂ AlSi ₃ O ₁₀)	3
Anhydrite	CaSO ₄	4	-	-	-
Cristobalite	SiO ₂	6	-	-	-
Calcium Silicate Hydrate	Ca ₆ Si ₃ O ₁₂ H ₂ O	5	-	-	-
Calcium and Aluminum Sulphate Hydrated	Ca ₄ Al ₂ S ₂ O ₉ H ₂ O	3	-	-	-

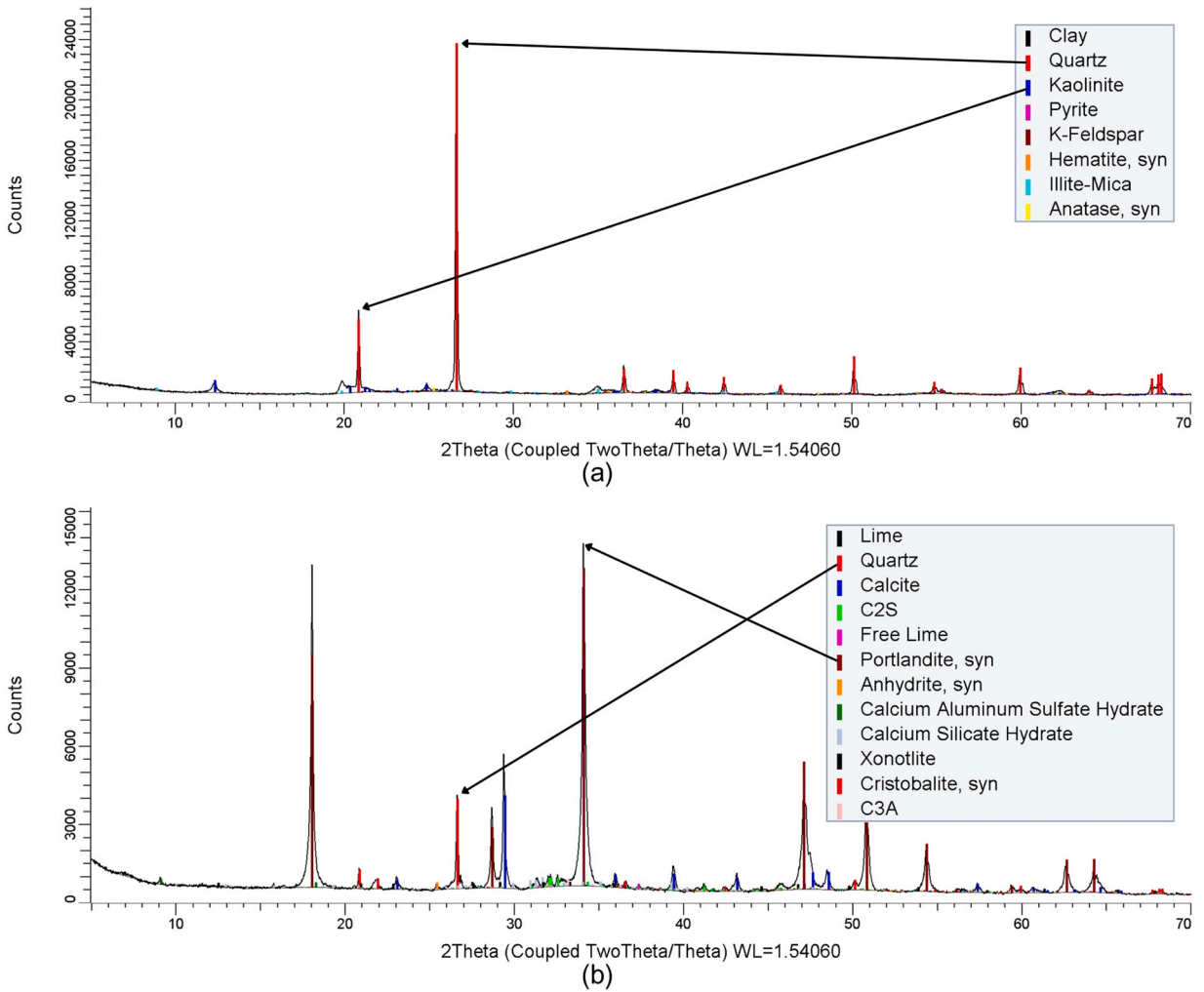


Fig. 10. Disfractograms.

EMS-15, EMS-45, EMS-30, and EMS-42 did not present DC. Phenomenon caused by the % of CMC added, which exceeded 50%. In contrast, EMS-35, EMS-2, EMS-4, EMS-39, EMS-11, and EMS-33 presented high DC. Phenomenon caused by high LM content.

Fig. 12 presents the reference pattern applied in the research to consider the DC of CM and EMS. The DC that were taken into account when assessing particle detachment are illustrated.

3.7. Density, volume loss, drying shrinkage and moisture absorption

The EMS-48 reported an increase in density (GD) of 50.96%, being the highest result obtained. Similarly, it reported the highest figure in LV 54.93%. This characteristic is attributed to the effect of the equal distribution of additions as described by Francesca Stazi et al., [44].

On the contrary, the EMS-33 registered a considerable loss of DY with -27.26%, the lowest result corresponding to LV 22.26% and DS 6.70%. Phenomenon attributed to LM being the only component added. Similar results were reported by Dwivedi and Gupta, who concluded that the combination of CL and LM can reduce the drying shrinkage of the mixes by 40–58% [45].

The addition of 50% CAS and LM showed 26.14% LV. Similar characteristics reported by the study conducted by J. M. de Souza et al., where the combination of CAS and cementitious material reduced the LV of EMS with additions of 6% wwt and 12.6%wt. However, in the study conducted, CAS was included in liquid form, since the CAS water used was residual CAS from flour production [46].

The EMS-48 reported the highest result with respect to DS with 20.50%. Phenomenon underpinning GD. EMS-33 reported the lowest DS result with 6.70%. Result ranking the EMS-33 as the most stable EMS with respect to LV. Stability offered by LM due to its binding properties and interaction with CMX conclusion made by Barbero-Barrera et al., [47].

EMS-15, EMS-45, EMS-30 and EMS-42 reported % DS between 11% and 15%. This result contrasts with the minimal GD obtained.

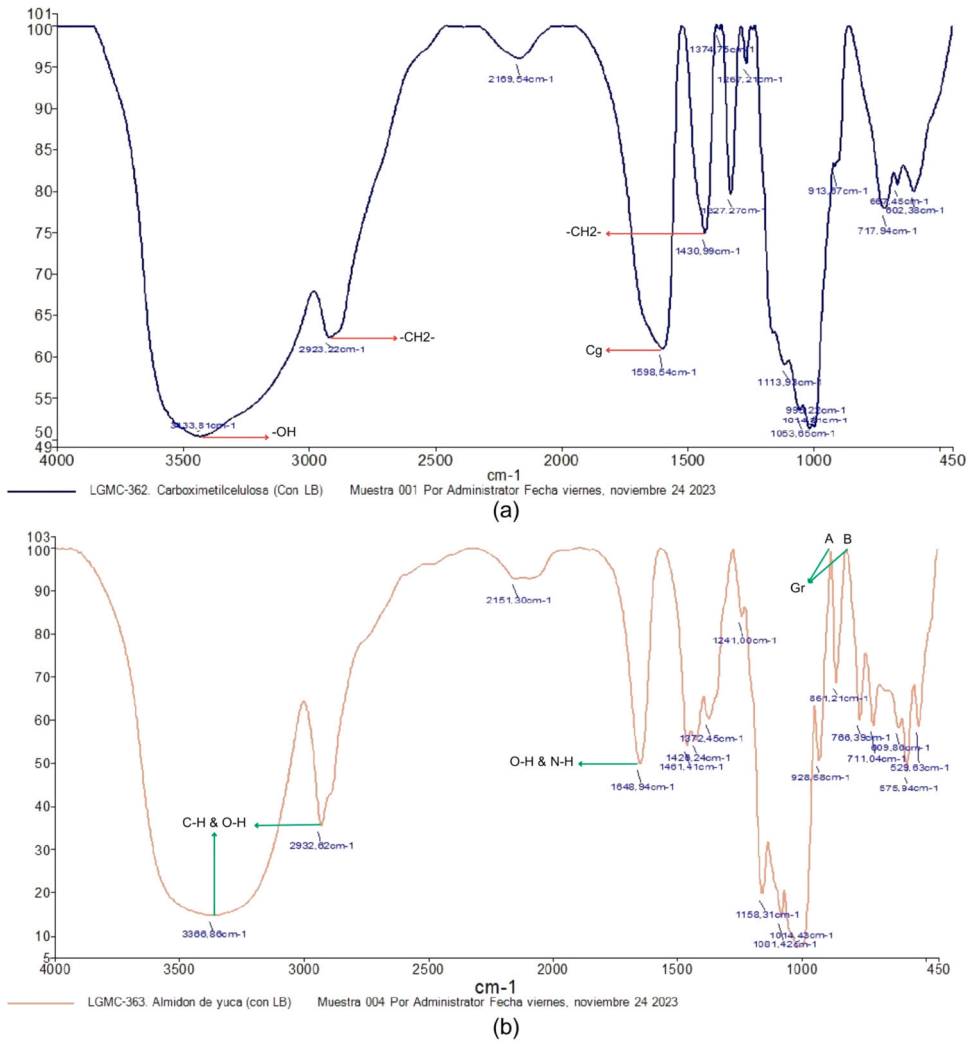


Fig. 11. FTIR CMC & CAS.

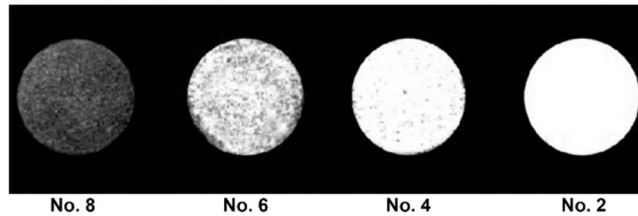


Fig. 12. Method A reference pattern NTC 1457-6 [31].

Property caused by particle coupling generated by the CMC.

EMS-38 with 8.87% and EMS-33 with 8.10% presented the highest % of MA. Characteristic attributed to the high contents of LM. The EMS-28 with 1.56% presented the lowest % of MA. Characteristic that contrasts with EMS-38 and EMS-33 due to the absence of LM. EMS with high CMC contents showed % MA from 2% to 5%. Similar result reported by Ozhan and Erkal concluding that the addition of up to 16%/wt of CMC in MCM achieves considerable decrease in EMS permeability [48].

In contrast, Shao et al., used CMC for hydraulic soil improvement, due to its ability to absorb and encapsulate large amounts of water. The study concluded that CMC could improve the water holding capacity of soils. Characteristics that demonstrate the versatility of the organic material and the diversity of its applications depending on the application interest [49].

3.8. Mechanical behavior

The EMS-48 had the highest CS with 115.26 kg of force/cm² (kgf/cm²). However, it obtained 23,61 kgf/cm² in FS. This phenomenon is due to the considerable GD that weakened its FS behavior. GD which contrasts with the reference study by Y. Trambitski et al., where it is indicated that the use of wheat and barley fibers in MCM reduced its DY by 34%. Special feature provided by the inclusion of vegetable fibers in MCM [50]. EMS-2 and EMS-33 presented the lowest data with respect to CS and FS. Phenomenon attributed to the lack of particle coupling due to the absence of CMC.

The CS and FS of EMS-2 and EMS-33 contrast with the study of LM mortars with CL additions performed by Simon Jayasingh & Jennie Bebe. Study that described the considerable increase in CS and FS of EMS. However, the research used LM as a matrix and CL as an addition [51]. A similar effect was reported by Hee-Young Hwang et al., indicating that, depending on the characteristics and origin of the additives, considerable effects on EMS properties are achieved [52].

Particular phenomena were presented by EMS-15, EMS-45, EMS-30 and EMS-42, which in addition to obtaining null DC and similar % DS, reported CS between 80 kgf/cm² close to 90 kgf/cm². Among these EMS, the EMS-30 stood out, showing similarities in CS and FS.

Fig. 13 shows the results in % obtained for the physical tests GD, LV, DS, and MA. The relationship between LV and GD of EMS-40 and EMS-24 can be identified. The closeness in % of GD, DS and MA in EMS-2 and EMS-4 is shown in Fig. 13a.

The CS and FS of the CM and EMS are shown with the CM as the baseline reference. The favorable performance of EMS with CMC addition is identified. The low FS performance of EMS with LM addition is shown. The minimal difference in the CS and FS peaks corresponding to the EMS-30 and EMS-42 Fig. 13b.

Table 5 groups the results of the CM and EMS physicochemical tests. The DC is indicated with an X. The results of the % of GD, LV, DS, and MA are presented. The results corresponding to CS and FS in kgf/cm² are shown.

3.9. SEM

The SEM observations were able to describe the phenomena that caused the physicochemical behavior of the CM and EMS.

Fig. 14 shows the observations made at CM, EMS-33, EMS-15 and EMS-11. The SEM image of the CM is presented. Heterogeneous and amorphous microstructure of Portlandite (Pt) is identified. Dense areas (Dd) are indicated in which the homogeneous compaction produced by the hydration of the finest CL particles is evident. Particle compaction is present, which limited the DS. Particle separation (Ps) is present, a characteristic that notably favors its detachment, as indicated by the results of the DC test Fig. 14a. Similar characteristics were found in the research conducted by Khorasani & Kabir where they studied the efficacy of CL mortars for use as plastering [35].

EMS-33 observation shown. Mixture with addition of 100% of LM. Dd and porous areas (Pa) that decrease their CS and FS and avoid their DS are identified. As in the CM, there is a lack of particle coupling. There are cavities (C) caused by detached particles Fig. 14b. This type of particle separation was reported in the research conducted by Morsy et al., where they incorporated rice straw ash and sodium hydroxide in MCM [53].

The observation made to the EMS-15 is shown. Mixture to which only CMC has been added. Dd is present due to particle coupling caused by CMC which prevented DC. Pores (P) caused by the encapsulation of MW by the CMC are identified. Characteristic that favored its LV. Undissolved CMC residues are also present in Fig. 14c. Similar particle coupling was obtained with the adobe elaborated in the research carried out by Abid et al., where other elements of natural origin were incorporated to the MCM [54].

The observation made to the EMS-11 whose addition was 100% of CAS is presented. Multiple cracks (F) are shown, which

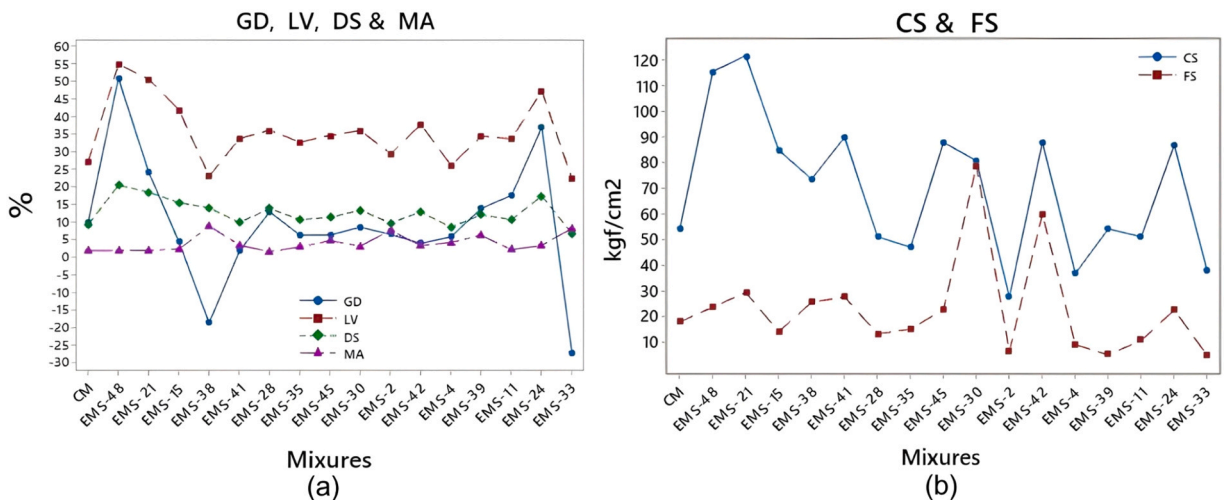


Fig. 13. CM & EMS physicochemical test results.

Table 5
CM and EMS physicochemical test results.

Mixures	Physical tests								Mechanical test	
	DC				%				kgf/cm^2	
	No. 8	No. 6	No. 4	No. 2	GD	LV	DS	MA	CS	FS
CM	-	-	X	-	10,11	27,24	9,31	1,76	54,06	17,85
EMS-48	-	X	-	-	50,96	54,93	20,50	1,84	115,26	23,61
EMS-21	-	X	-	-	24,24	50,73	18,55	1,94	121,38	29,33
EMS-15	X	-	-	-	4,40	41,93	15,55	2,32	84,66	14,08
EMS-38	-	-	X	-	-18,69	23,09	14,06	8,87	73,44	25,55
EMS-41	-	X	-	-	1,73	33,80	9,87	3,36	89,76	27,54
EMS-28	-	X	-	-	12,94	36,16	13,87	1,56	51	13,18
EMS-35	-	-	-	X	6,33	32,75	10,70	2,9	46,92	15,10
EMS-45	X	-	-	-	6,33	34,69	11,35	4,69	87,72	22,70
EMS-30	X	-	-	-	8,58	36,07	13,40	3,14	80,58	78,50
EMS-2	X	-	-	X	6,50	29,45	9,77	7,6	27,54	6,53
EMS-42	X	-	-	-	3,94	37,81	12,92	3,31	87,72	59,82
EMS-4	-	-	-	X	5,82	26,14	8,56	4,13	36,72	9,03
EMS-39	-	-	-	X	13,94	34,47	12,09	6,27	54,06	5,05
EMS-11	-	-	-	X	17,61	33,74	10,70	2,13	51	10,66
EMS-24	-	-	X	-	37,02	47,39	17,47	3,26	86,7	22,54
EMS-33	-	-	-	X	-27,26	22,26	6,70	8,10	37,74	4,79

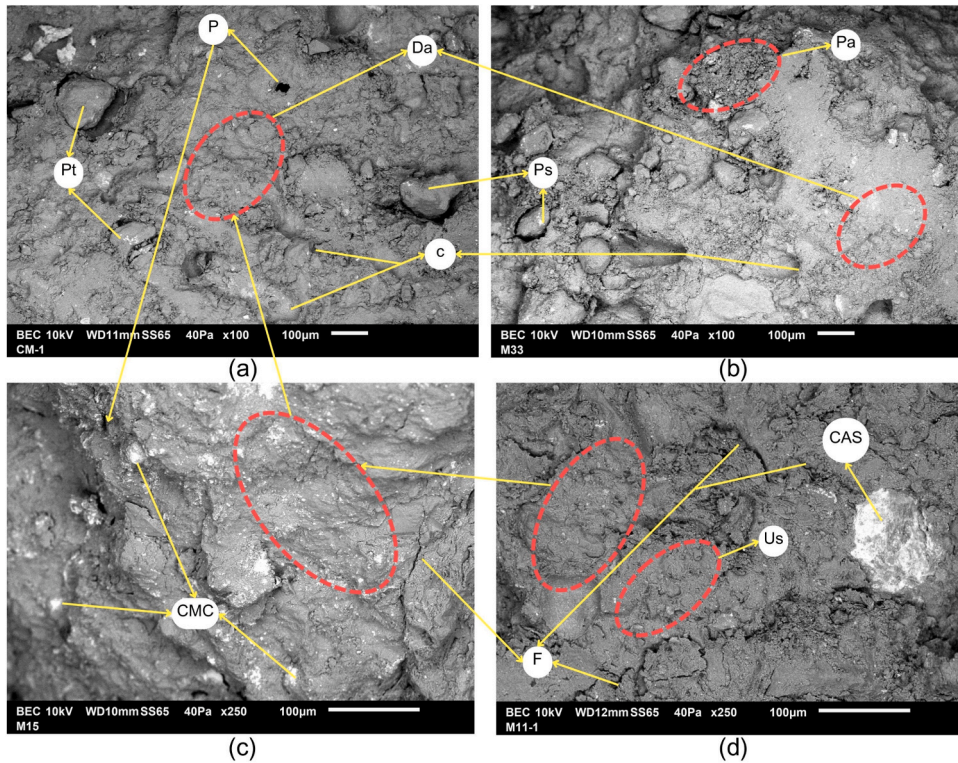


Fig. 14. SEM observations CM, M-33, M-15, and M-11.

weakened the SP and prevented better results in CS and FS. Dd and undulations (Us) are present, which favored DC. Encapsulation of CAS also occurs due to lack of dissolution Fig. 14d. Some of these phenomena were reported in the review article published by Avila et al., when they mentioned the incorporation of some plant elements in MCM [55].

EDS mapping it was possible to perform a microanalysis of the elemental chemical dispersion in the different regions of the EMS. Fig. 15 shows the Carbon (C) content in a scattered way Fig. 15a. Oxygen (O) content Fig. 15b. Silica (Si) content Fig. 15c. Aluminum (Al) Content Fig. 15d.

Fig. 16 shows the chemical interaction of the components in the EMS. EMS-48 shows the homogeneously dispersed (Hd) of LM, CAS and CMC in CMX. Characteristic that favoured CS due to the particle coupling generated by the addition of CMC and CAS Fig. 16a.

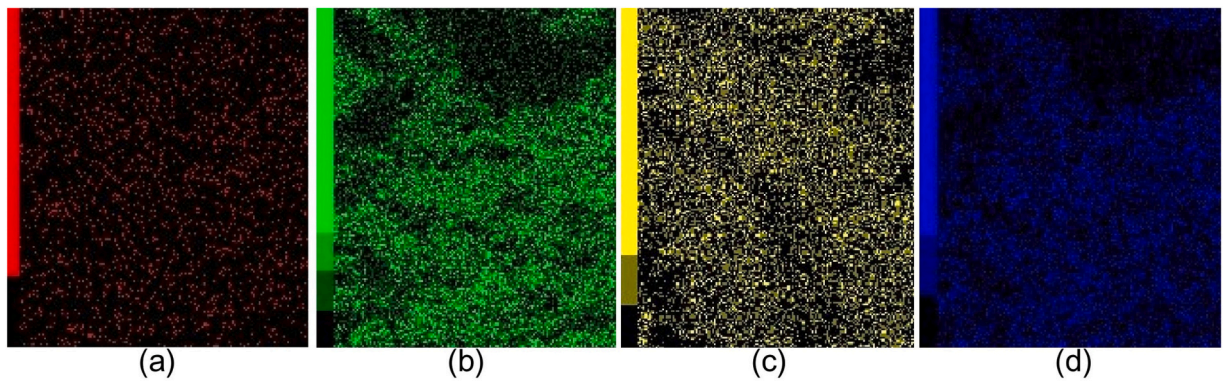


Fig. 15. EDS mapping.

EMS-2 shows the isolated concentration of O and C. Predominant elements in organic compounds such as CAS. Characteristic that considerably reduced its CS by increasing the DC. Phenomenon caused by the lack of CMC and the scarce interaction of CAS with Al and Si present in the LM Fig. 16b. EMS-30 shows compact O and C concentrations corresponding to the predominant CMC. Binding characteristics of the organic material that caused its perfect coupling with CAS and CL. The null DC favoured its mechanical resistance, obtaining similar results in CS and FS Fig. 16c. EMS-42 shows the coupling of Al and Si of the LM with the C present in the CMC. Phenomenon that caused similar characteristics to EMS-30 Fig. 16d.

Predominant Si interactions were observed with quartz being the mineral that constitutes quartz. The presence of Portlandite was observed, being the calcium hydroxide present in the LM. The presence of the element O present in the hydroxyl groups of CMC and CAS was observed. Interactions that were presented as Hd in Fig. 16a. However, Fig. 16b shows areas with a lack of interaction increasing DC. In contrast, Fig. 16c shows compact zones due to the encapsulation of the MW by the CMC. Phenomenon that avoids DC. Similarly, Fig. 16d shows the interaction of Si and Al present in CL with calcium hydroxide from LM and O from CMC enhancing particle adhesion.

4. Conclusions

4.1. DC

It is important to know the DC of the EMS with CMX to correctly select the EMS with the best performance according to the application or performance desired with the element or mixture to be constituted. Lack of knowledge about DC leads to problems in the installation of construction elements when applying plaster or covering layers due to difficulties in adherence between elements.

The detachment of particles leads to premature deterioration of construction elements with CMX. They can also cause respiratory problems in inhabitants. The above, in the case of the application of EMS with CMX in the elaboration of structural elements that do not contemplate coatings.

With the above, the research concludes that the EMS 15, EMS-45, EMS-30 and EMS-42 guarantee the fixation and coupling of particles avoiding their detachment. Characteristic attributed to the %wt of CMC added. The mixtures were selected because the DC test showed that they did not release particles. This phenomenon is caused by the hydrophilic property of CMC that allows the generation of gels using an adhesive behavior that helps to capture the clay particles avoiding their detachment. Regarding the results reported in the CS and FS, these could be improved by other additions or simply by incorporating vegetable fibers at the time of forming composites with compostable characteristics - Green Composites.

In future research to improve the properties of MCM, other materials of plant origin with renewable characteristics could be incorporated to act as coupling agents in order to guarantee the adhesion of the particles and prevent their detachment.

4.2. DY, LV, DS & MA

Identifying changes in DY, LV and DS of EMS with CMX allows predicting behavior under external stress and climatic conditions. In the same way, it is possible to estimate the appearance of cracks to implement actions to mitigate these phenomena when incorporating EMS in construction projects.

In this sense, the addition of LM favored the reduction of this phenomenon. Consequently, EMS-38, EMS-35, EMS-2 and EMS-33 recorded lower values for LV due to the interaction of the calcium hydroxide present in the LM with the Al, Si, and O content of the CL, which enables a pozzolanic reaction through hydration with the MW. Characteristic that allows the stabilization of MCM avoiding volumetric changes. However, the CS and FS were not favorable. Mechanical characteristics that can be improved by the inclusion of fine aggregate or plant fibers reinforcement in order to increase the strength of the composite.

In contrast, the high LM contents in EMS-38, EMS-2 and EMS-33 favored the MA. Phenomenon caused by the need for hydration of unstabilized LM. This situation makes it necessary to add components that guarantee the protection of the EMS against moisture due to

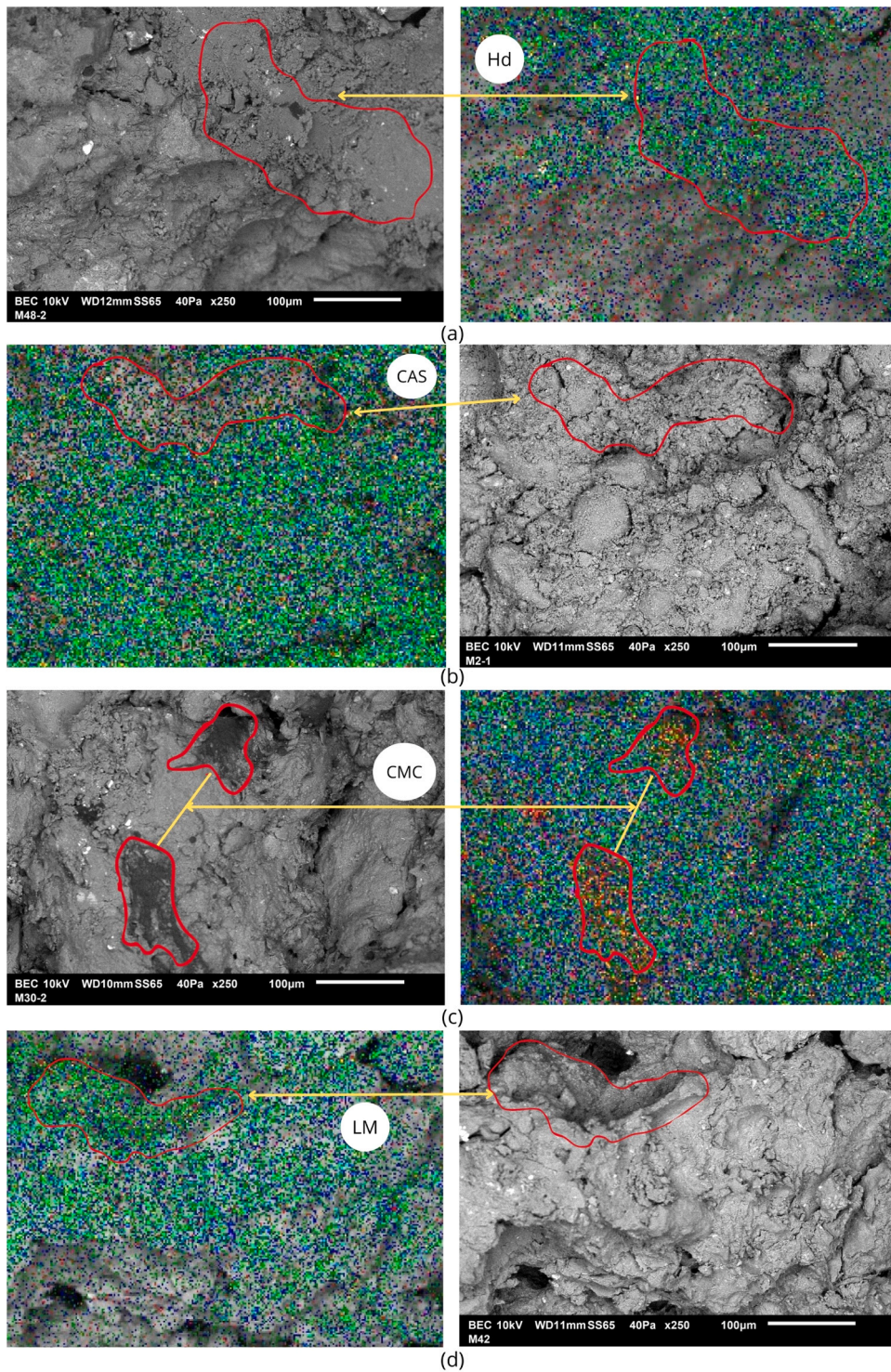


Fig. 16. Chemical interaction of components.

the exothermic properties of LM.

The research results generate a starting point for future research whose main objective is the stabilization of CL for its implementation as a construction material.

4.3. CS & FS

The search for methods that increase the CS and FS in materials is undoubtedly one of the key points in research to ensure the design of materials with high performance and functionality. However, the industrial sector, and especially the construction sector, makes use of temporary materials with minimal mechanical requirements.

In this sense, the EMS-48 with similar distribution of additions recorded the highest CS with the greatest increase in density, considerably affecting its FS. In contrast to the EMS with CMC additions that in addition to presenting null DC recorded CS between 80 kgf/cm^2 and 90 kgf/cm^2 . Reason justifying the selection of the most favorable EMS according to the technical requirements requested.

Improving the mechanical behavior of MCMs is the main objective of research in order to scientifically justify the use of soil in construction projects. However, the other physical properties of MCMs must be taken into account to ensure the durability of the resulting material.

4.4. SEM

SEM observations with EDS mapping allowed the identification of the interaction of the components in EMS (see Fig. 16). The influence of the additions in similar % on the favorable CS was determined. However, unfavorable phenomena occurred in LV, DS, and FS. The particle coupling capacity produced by the addition of CMC was identified. The mechanical disadvantages provided by the addition of LM were observed. However, LM prevents LV and DS. It was possible to demonstrate the favorable interaction of CAS and CMC, a combination that, in addition to improving CS and FS, produced a favorable DC.

In general, it is concluded that the additions favored the increase of MCM physicochemical properties. By reviewing the results obtained, it would be possible to select the appropriate EMS for implementation in future projects, considering the final performance intended with the proposed new material. Remembering that materials with high mechanical requirements are not always required.

The results obtained identify the influence of LC, CAS, and CMC on the physicochemical properties of MCM. The comparison of results between CM and EMS facilitated the identification of the EMS with the best characteristics. However, by analyzing the results, optimal mixtures can be selected for the implementation of ancient construction techniques in the construction of modern projects.

These types of research reports highlight the importance of research aimed at improving the physicochemical characteristics of MCM. However, the multiple combinations of additions in EMS may contrast with the results obtained in others research. This is due to the use of local materials that may have particular physical, chemical or mineralogical characteristics in their compositions. Such is the case with the use of organic materials.

On the other hand, the use of alternative materials may increase the costs of the resulting mixtures due to the implementation of plant elements obtained from complex processes. In this sense, the economic evaluation of the use of substitute materials is an important factor at the time of their implementation. However, the research results generate interesting data to initiate new research with plant elements with similar characteristics compared to those evaluated.

For this reason, further research is needed to evaluate local materials for their implementation as substitute materials in the construction sector, seeking the creation of totally biodegradable materials and low-cost.

Funding

This research received no external funding.

CRedit authorship contribution statement

Alfonso Cobo Escamilla: Writing – review & editing, Supervision, Methodology, Formal analysis. **Humberto Varum:** Writing – review & editing, Supervision, Methodology. **Oswaldo Hurtado-Figueroa:** Writing – original draft, Validation, Methodology, Investigation, Formal analysis, Conceptualization. **Romel Jesus Gallardo Amaya:** Writing – review & editing, Supervision.

Declaration of Competing Interest

The authors declare that they have no known competing financial interests or personal relationships that could have appeared to influence the work reported in this paper.

Data availability

Some or all data generated or used during the study are available from the corresponding author by request.

Acknowledgement

The authors are grateful for the laboratories; LABMAC—SENA—Centro C.I.E.S Regional Norte de Santander, Biotechnology and Nanotechnology laboratory—Tecnoparque SENA—Nodo—Cucuta, Textile and Leather Manufacturing SENA—Bogotá, LaC-GMC

Universidad del Valle, GMAS— S.A.S—Bogota.

References

- [1] J. Dsilva, S. Zarmukhambetova, J. Locke, Assessment of building materials in the construction sector: a case study using life cycle assessment approach to achieve the circular economy, *Heliyon* 9 (2023) e20404, <https://doi.org/10.1016/j.heliyon.2023.e20404>.
- [2] S. Barbhuiya, B. Bhusan, Life Cycle Assessment of construction materials: Methodologies, applications and future directions for sustainable decision-making, *Case Stud. Constr. Mater.* 19 (2023) e02326, <https://doi.org/10.1016/j.cscm.2023.e02326>.
- [3] M. Franciosi, V. Savino, L. Lanzoni, A.M. Tarantino, M. Viviani, Changing the approach to sustainable constructions: an adaptive mix-design calibration process for earth composite materials, *Compos. Struct.* 319 (2023) 117143, <https://doi.org/10.1016/j.compstruct.2023.117143>.
- [4] I. Ijeoma, A. Peter, A.P. Onwualu, A.B.O. Soboyejo, Materials Mechanical behaviour of lateritic soil stabilized with bone ash and hydrated lime for sustainable building applications, *Case Stud. Constr. Mater.* 12 (2020) e00331, <https://doi.org/10.1016/j.cscm.2020.e00331>.
- [5] P. Kasinikota, D.D. Tripura, Prediction of physical-mechanical properties of hollow interlocking compressed unstabilized and stabilized earth blocks at different moisture conditions using ultrasonic pulse velocity, *J. Build. Eng.* 48 (2022) 103961, <https://doi.org/10.1016/j.jobe.2021.103961>.
- [6] D. Thompson, C. Augarde, J.P. Osorio, A review of current construction guidelines to inform the design of rammed earth houses in seismically active zones, *J. Build. Eng.* 54 (2022) 104666, <https://doi.org/10.1016/j.jobe.2022.104666>.
- [7] M. Gomaa, S. Schade, D. Wen, Y. Min, Automation in rammed earth construction for industry 4.0: precedent work, current progress and future prospect, *J. Clean. Prod.* 398 (2023) 136569, <https://doi.org/10.1016/j.jclepro.2023.136569>.
- [8] J. Saliba, A. Schultz, J. Moye, K. Pistol, Mechanical characterization and durability of earth blocks, *Mater. Today Proc.* (2023), <https://doi.org/10.1016/j.matpr.2023.06.165>.
- [9] A. Thennarasan Latha, B. Murugesan, B. Skariah Thomas, Compressed earth block reinforced with sisal fiber and stabilized with cement: manual compaction procedure and influence of addition on mechanical properties, *Mater. Today Proc.* (2023), <https://doi.org/10.1016/j.matpr.2023.04.373>.
- [10] R.I. Khan, M. Intesarul, A. Tahsin, W. Ashraf, Multiscale performance and environmental impact assessment of slag and Portland blended cement for optimum carbonation curing, *Cement* 14 (2023) 100088, <https://doi.org/10.1016/j.cement.2023.100088>.
- [11] C.R. Ganesh, J. Sumalatha, K.S. Sreekeshava, K. Sharath, Experimental study on strength behaviour of geofibre reinforced stabilized mud blocks using industrial by-products, *Mater. Today Proc.* (2023), <https://doi.org/10.1016/j.matpr.2023.04.045>.
- [12] A. Laveglia, L. Sambataro, N. Ukrainczyk, T. Oertel, N. De Belie, E. Koenders, How to improve the cradle-to-gate environmental and economic sustainability in lime-based construction materials? Answers from a EU Proportion of Sensitive Indicators, *Dev. Built Environ.* 15 (2023) 100186, <https://doi.org/10.1016/j.dibe.2023.100186>.
- [13] S. Paul, M.S. Islam, T.E. Elahi, Potential of waste rice husk ash and cement in making compressed stabilized earth blocks: strength, durability and life cycle assessment, *J. Build. Eng.* 73 (2023) 106727, <https://doi.org/10.1016/j.jobe.2023.106727>.
- [14] J. Zhai, I.T. Burke, D.I. Stewart, Potential reuse options for biomass combustion ash as affected by the persistent organic pollutants (POPs) content, *J. Hazard. Mater. Adv.* 5 (2022) 100038, <https://doi.org/10.1016/j.hazadv.2021.100038>.
- [15] S.S. Aninda, M.S. Islam, Effectiveness of waste concrete powder in fabricating compressed stabilized earth blocks: strength, durability and thermal assessment, *J. Build. Eng.* 80 (2023) 107989, <https://doi.org/10.1016/j.jobe.2023.107989>.
- [16] A. Kul, B. Furkan, E. Ozelicli, M. Faruk, H. Ulugol, G. Yildirim, M. Sahmaran, Characterization and life cycle assessment of geopolymer mortars with masonry units and recycled concrete aggregates assorted from construction and demolition waste, *J. Build. Eng.* 78 (2023) 107546, <https://doi.org/10.1016/j.jobe.2023.107546>.
- [17] R.H. Sadok, N.B. Belaribi, R. Mazouzi, F.H. Sadok, Life cycle assessment of cementitious materials based on calcined sediments from Chorfa II dam for low carbon binders as sustainable building materials, *Sci. Total Environ.* 826 (2022) 154077, <https://doi.org/10.1016/j.scitotenv.2022.154077>.
- [18] R. Panagiotou, M.A. Kyriakides, R. Illampas, I. Ioannou, An experimental approach for the investigation of the performance of non-stabilized Compressed Earth Blocks (CEBs) against water-mediated weathering, *J. Cult. Herit.* 57 (2022) 184–193, <https://doi.org/10.1016/j.culher.2022.08.009>.
- [19] O. Hurtado-Figueroa, Alfonso Cobo Escamilla, Humberto Varum, The mercerization process and its impact on rice straw surface topography, *Buildings* 13 (2023) 1–29, <https://doi.org/10.3390/buildings13071573>.
- [20] M. Costi de Castrillo, I. Ioannou, M. Philokyprou, Reproduction of traditional adobes using varying percentage contents of straw and sawdust, *Constr. Build. Mater.* 294 (2021) 123516, <https://doi.org/10.1016/j.conbuildmat.2021.123516>.
- [21] Y. Wu, Jia-le Zhou, Xin-yue Zhou, Z. Hu, Q. Cai, Shi-guan Yang, Q. Lu, Site selection of crop straw cogeneration project under intuitionistic fuzzy environment: A four-stage decision framework from the perspective of circular economy, *J. Clean. Prod.* 395 (2023) 136431, <https://doi.org/10.1016/j.jclepro.2023.136431>.
- [22] S. Barbhuiya, B. Bhusan, Life Cycle Assessment of construction materials: Methodologies, applications and future directions for sustainable decision-making, *Case Stud. Constr. Mater.* 19 (2023) e02326, <https://doi.org/10.1016/j.cscm.2023.e02326>.
- [23] M. Abu, B. Kumar, A. Farouk, S. Pandey, A. Hussain, A. Ragab, S. Alvi, S.M. Mozammil, Assessment of the mechanical and durability characteristics of bio-mineralized *Bacillus subtilis* self-healing concrete blended with hydrated lime and brick powder, *Case Stud. Constr. Mater.* 19 (2023) e02672, <https://doi.org/10.1016/j.cscm.2023.e02672>.
- [24] A.N. Adazabra, G. Viruthagiri, S.A. Sulemana, J. Yirijor, Valorising cassava pomace biosolid in fired clay bricks production: physical, mechanical and thermal evaluation, *Mater. Chem. Phys.* 309 (2023) 128402, <https://doi.org/10.1016/j.matchemphys.2023.128402>.
- [25] P. Sirajudheen, P. Karthikeyan, S. Vigneshwaran, S. Meenakshi, Synthesis and characterization of La(III) supported carboxymethylcellulose-clay composite for toxic dyes removal: Evaluation of adsorption kinetics, isotherms and thermodynamics, *Int. J. Biol. Macromol.* 161 (2020) 1117–1126, <https://doi.org/10.1016/j.ijbiomac.2020.06.103>.
- [26] ISO 13320:2020, Particle size analysis Laser diffraction methods. <https://www.iso.org/standard/69111.html>, 2020 (Accessed 17 November 2023).
- [27] INV-125-13, Determinación del límite líquido de los suelos. <https://www.da-lab.co/wp-content/uploads/2021/04/INV-125-13.pdf>, 2021 (Accessed 15 May 2023).
- [28] INV-126-13, Límite plástico e índice de plasticidad de los suelos. <https://www.da-lab.co/wp-content/uploads/2021/04/INV-126-13.pdf>, 2021 (Accessed 18 May 2023).
- [29] M. Lagouin, J.-E. Aubert, A. Laborel-Préneron, C. Magniont, Influence of chemical, mineralogical and geotechnical characteristics of soil on earthen plaster properties, *Constr. Build. Mater.* 304 (2021) 124339, <https://doi.org/10.1016/j.conbuildmat.2021.124339>.
- [30] J.A. Cottrell, M. Ali, A. Tatari, D.B. Martinson, Effects of fibre moisture content on the mechanical properties of jute reinforced compressed earth composites, *Constr. Build. Mater.* 373 (2023) 130848, <https://doi.org/10.1016/j.conbuildmat.2023.130848>.
- [31] NTC 1457-6:2017, Métodos de ensayo para evaluar el grado de entzamiento de películas de pintura exterior. <https://tienda.icontec.org/gp-metodos-de-ensayo-para-evaluar-el-grado-de-entzamiento-de-peliculas-de-pintura-exterior-ntc1457-6-2017.html>, 2017 (Accessed 21 May 2023).
- [32] NTC-220-2022, Cementos. Determinación de la resistencia de morteros de cemento hidráulico a la compresión, usando cubos de 50 mm o 2 pulgadas de lado. <https://tienda.icontec.org/gp-ntc-cementos-determinacion-de-la-resistencia-de-morteros-de-cemento-hidraulico-a-la-compresion-usando-cubos-de-50-mm-o-2-pulgadas-de-lado-ntc220-2022.html>, 2022 (Accessed 12 June 2023).
- [33] M. Costi, D. Castrillo, I. Ioannou, M. Philokyprou, Reproduction of traditional adobes using varying percentage contents of straw and sawdust, *Constr. Build. Mater.* 294 (2021) 123516, <https://doi.org/10.1016/j.conbuildmat.2021.123516>.
- [34] NTC-120-2022, Cementos. Método de ensayo para determinar la resistencia a la flexión de morteros de cemento hidráulico. <https://tienda.icontec.org/gp-ntc-cementos-metodo-de-ensayo-para-determinar-la-resistencia-a-la-flexion-de-morteros-de-cemento-hidraulico-ntc120-2022.html>, 2022 (Accessed 12 June 2023).
- [35] F.F. Khorasani, M.Z. Kabir, Experimental study on the effectiveness of short fiber reinforced clay mortars and plasters on the mechanical behavior of adobe masonry walls, *Case Stud. Constr. Mater.* 16 (2022) e00918, <https://doi.org/10.1016/j.cscm.2022.e00918>.

- [36] M.V. Vasić, L.L. Pezo, Z. Radojević, Optimization of adobe clay bricks based on the raw material properties (mathematical analysis), *Constr. Build. Mater.* 244 (2020) 118342, <https://doi.org/10.1016/j.conbuildmat.2020.118342>.
- [37] USCS, Unified Soil Classification System. <https://transportation.org/technical-training-solutions/wp-content/uploads/sites/64/2023/02/AT-TC3CN025-18-T1-JA03-11.pdf>, 2023 (Retrieved Feb 18, 2023).
- [38] T.T. Stanislas, G.C. Komadja, Y.R. Nafu, A.A. Mahamat, P.W.H. Mejouyo, J.F. Tendo, E. Njeugna, P.A. Onwualu, H.S. Junior, Potential of raffia nanofibrillated cellulose as a reinforcement in extruded earth-based materials, *Case Stud. Constr. Mater.* 16 (2022) e00926, <https://doi.org/10.1016/j.cscm.2022.e00926>.
- [39] N. Isak, K. Khaxhiu, E. Behrami, A. Andoni, A comparative study of the adsorption and desorption process of selected natural Albanian clays toward methomyl and dimethoate pesticides, *J. Environ. Manag.* 346 (2023) 118989, <https://doi.org/10.1016/j.jenvman.2023.118989>.
- [40] Y. Bali, A. Kriker, Y. Abimouloud, S. Bouzouaid, Improving thermal insulation of fired earth bricks with alfa plant and glass powder additives: Effects on thermo-physical and mechanical properties, *Case Stud. Therm. Eng.* 53 (2024) 103778, <https://doi.org/10.1016/j.csite.2023.103778>.
- [41] T.B. Su-cadirci, J. Calabria-holley, C. Ince, R. James, Freeze-thaw resistance of pozzolanic hydrated lime mortars, *Constr. Build. Mater.* 394 (2023) 131993, <https://doi.org/10.1016/j.conbuildmat.2023.131993>.
- [42] D.C.M. Ferreira, G. Molina, F.M. Pelissari, Biodegradable trays based on cassava starch blended with agroindustrial residues, *Compos. Part B: Eng.* 183 (2020) 107682, <https://doi.org/10.1016/j.compositesb.2019.107682>.
- [43] V. Thathsarane, L. Moghaddam, Z. Welsh, T. Wang, H. Xiao, A. Karim, Extraction and characterisation of starch from cassava (*Manihot esculenta*), *LWT* 182 (2023) 114787, <https://doi.org/10.1016/j.lwt.2023.114787>.
- [44] F. Stazi, N. Pierandrei, C. Di, F. Tittarelli, Case studies in construction materials experimental evaluation of natural hydraulic lime renders with nanoclay and nanolime to protect raw earth building surfaces, *Case Stud. Constr. Mater.* 17 (2022) e01564, <https://doi.org/10.1016/j.cscm.2022.e01564>.
- [45] A. Dwivedi, S. Gupta, Influence of carbon sequestration in natural clay on engineering properties of cement-lime stabilized soil mortars, *Dev. Built Environ.* 16 (2023) 100270, <https://doi.org/10.1016/j.dibe.2023.100270>.
- [46] J.M. de Souza, R. Barbosa, J. Batista, V. Monteiro, S. do Rêgo, L. de Figueiredo, W. Acchar, Mechanical and durability properties of compressed stabilized earth brick produced with cassava wastewater, *J. Build. Eng.* 44 (2021) 103290, <https://doi.org/10.1016/j.jobe.2021.103290>.
- [47] M.M. Barbero-barrera, F. Jové-sandoval, S. González, Assessment of the effect of natural hydraulic lime on the stabilisation of compressed earth blocks, *Constr. Build. Mater.* 260 (2020) 119877, <https://doi.org/10.1016/j.conbuildmat.2020.119877>.
- [48] H.O. Ozhan, A. Erkal, Internal erosion and permeability of Na CMC-treated and PAM-treated geosynthetic clay liners, *Geotext. Geomembr.* 51 (2023) 17–27, <https://doi.org/10.1016/j.geotextmem.2023.08.002>.
- [49] F. Shao, S. Zeng, Q. Wang, W. Tao, J. Wu, L. Su, H. Yan, Y. Zhang, S. Lin, Synergistic effects of biochar and carboxymethyl cellulose sodium (CMC) applications on improving water retention and aggregate stability in desert soils, *J. Environ. Manag.* 331 (2023) 117305, <https://doi.org/10.1016/j.jenvman.2023.117305>.
- [50] Y. Trambitski, O. Kizinievic, V. Kizinievic, Modification of clay materials with retrograded starch hydrogel, *Constr. Build. Mater.* 314 (2022) 125619, <https://doi.org/10.1016/j.conbuildmat.2021.125619>.
- [51] S. Jayasingh, J. Baby, Influence of organic addition on strength and durability of lime mortar prepared with clay aggregate, *Mater. Today Proc.* 64 (2022) 1006–1013, <https://doi.org/10.1016/j.matpr.2022.05.088>.
- [52] H.-Y. Hwang, Y.-H. Kwon, S.-G. Hong, S.-H. Kang, Comparative study of effects of natural organic additives and cellulose ether on properties of lime-clay mortars, *J. Build. Eng.* 48 (2022) 103972, <https://doi.org/10.1016/j.jobe.2021.103972>.
- [53] M.I. Morsy, K.A. Alakeel, A.E. Ahmed, A.M. Abba, A.I. Omara, N.R. Abdelsalam, H.H. Emaish, Recycling rice straw ash to produce low thermal conductivity and moisture-resistant geopolymer adobe bricks, 2022, *Saudi J. B Sci.* 29 (2022) 3759–3771, <https://doi.org/10.1016/j.sjbs.2022.02.046>.
- [54] R. Abid, N. Kamoun, F. Jamoussi, H. El, Fabrication and properties of compressed earth brick from local Tunisian raw materials, *Boletín. la Soc. Española Cerámica Y. Vidr.* 61 (2021) 397–407, <https://doi.org/10.1016/j.bsecv.2021.02.001>.
- [55] F. Ávila, E. Puertas, R. Gallego, Characterization of the mechanical and physical properties of stabilized rammed earth: a review, *Constr. Build. Mater.* 325 (2022) 126693, <https://doi.org/10.1016/j.conbuildmat.2022.126693>.